Polymer 103 (2016) 214–223

Contents lists available at ScienceDirect

Polymer

journal homepage: www.elsevier.com/locate/polymer

Characterizations of PDMS-graft copolyimide membrane and the permselectivity of gases and aqueous organic mixtures

Cheol Min Yun [a, 1], Eiichi Akiyama [b], Takeshi Yamanobe [c], Hiroki Uehara [c], Yu Nagase [a, *]

[a] Graduate School of Science and Technology, Tokai University, 4-1-1 Kitakaname, Hiratsuka, Kanagawa 259-1292, Japan
[b] Sagami Chemical Research Institute, 2743-1 Hayakawa, Ayase, Kanagawa 252-1193, Japan
[c] Department of Chemistry and Chemical Biology, Gunma University, 1-5-1 Tenjin-cho, Kiryu, Gunma 376-8515, Japan

ARTICLE INFO

Article history:
Received 1 July 2016
Received in revised form
8 September 2016
Accepted 15 September 2016
Available online 15 September 2016

Keywords:
Polydimethylsiloxane
Polyimide
Graft copolymer
Gas permeability
Pervaporation
Thermal treatment

ABSTRACT

Polydimethylsiloxane (PDMS)-graft copolyimides were synthesized by polycondensation of 3,5-bis(4-aminophenoxy)benzyloxypropyl-terminated PDMS macromonomer with 4,4'-hexafluoroisopropylidene diphthalic anhydride (6FDA) followed by chemical imidization to investigate the effects of PDMS segment length of copolyimides on the membrane characteristics, the gas permeability and the pervaporation performance. The copolyimide membranes, which were prepared by solvent-casting method from the chloroform solutions, became insoluble in any solvents after the thermal treatment over 150 °C *in vacuo*. It was confirmed from TEM observation of these membranes that the phase separation of flexible PDMS domains and hard polyimide backbones. The gas permeability coefficients of copolyimide membranes were increased as the PDMS segment length increased, but decreased after thermal treatment at 200 °C. It would be due to the chain scission and the rearrangement of PDMS segments in the side chain to become a cross-linked structure, which make the membranes insoluble. From the results of pervaporation of dilute aqueous solutions of organics, it was found that the copolyimide membranes exhibited the excellent permselectivity toward several organics, such as ethanol, acetone, benzene, chloroform and dichloromethane with a high and stable permeation. Furthermore, it was confirmed that the removal of dichloromethane from its saturated aqueous solution was efficiently achieved by the pervaporation.

1. Introduction

Pervaporation is a promising membrane-based technique with potential savings in the cost of energy for the separation of liquid mixtures. One application of organic-permselective membrane is the removal and the recovery of volatile organic components (VOCs) and alcohols from waste fluid, industrial drainage or fermentation broths [1–5]. Especially, the water pollution due to VOCs has become a serious environmental problem. Polydimethylsiloxane (PDMS) has been known to show the high permselectivity for organic liquids against water in pervaporation, which is derived from the higher affinity for organic compounds than water with the high diffusivity [6–9]. To make a self-standing thin membrane, however, an improvement of the processability of PDMS is necessary, which would be achieved by the copolymerization with a high T_g or T_m component. Some researchers have investigated the improvement of processability of PDMS by controlling the chemical structure such as blends and block copolymers [10–16], although the PDMS content was limited to make a tough membrane. Meanwhile, the durability of membrane against VOCs is very important, because the organic components were concentrated in the membrane during permeation. Therefore, the PDMS rich polymer exhibiting high organic-permselectivity, processability and durability would be an ideal material to develop as a practical pervaporation membrane for the separation of VOCs.

From these points of view, we have attempted to synthesize novel PDMS-graft copolymers, the backbone structure of which consists of aromatic polyimide. Aromatic polyimides are well known to show the excellent mechanical strength, processability and the durability for several organic solvents, which have been studied for various applications in electronic devices, coating, composite materials and separation membranes [17–21]. In our

* Corresponding author.
E-mail address: yunagase@tokai-u.jp (Y. Nagase).
[1] Present address: LG Chem Research Park, 104-1 Moonji-dong, Yuseong-gu, Daejeon 305-738, South Korea.

http://dx.doi.org/10.1016/j.polymer.2016.09.044
0032-3861/

previous study, PDMS/polyimide graft copolymer was prepared by polycondensation of 3,5-diaminobenzyl-terminated PDMS macromonomer with aromatic diamine and dianhydride monomers [22–24]. Then, the obtained membrane exhibited the high organic-permselectivity with durability derived from the backbone component. However, the PDMS content was also limited due to the poor reactivity of 3,5-diaminobenzyl terminal group of the macromonomer, which should be copolymerized with other diamine monomers. In these years, we have developed the highly reactive PDMS macromonomers, which consisted of 3,5-bis(4-aminophenoxy)benzyloxypropyl-terminated PDMS and 3,5-bis(4-amino-3-methylphenoxy)benzyloxypropyl-terminated PDMS [25]. From the new PDMS macromonomers, PDMS-graft aromatic polymers could be obtained by polycondensation with terephthaloyl chloride, trimellitic anhydride chloride, 4,4'-hexafluoroisopropylidene diphthalic anhydride or 4,4'-oxydiphtahlic dianhydride [25–27]. Although the obtained polymers possessed the long PDMS segment in every repeating unit, the tough self-standing membranes could be prepared by a solvent casting method. Furthermore, the PDMS contents of PDMS-graft copolymers could be easily controlled by changing the PDMS segment length of the macromonomer [27]. In particular, the obtained PDMS-graft aromatic copolyimide based on 3,5-bis(4-aminophenoxy)benzyloxypropyl-terminated PDMS (BAPB-PDMS) and 4,4'-hexafluoroisopropylidene diphthalic anhydride (6FDA) exhibited the excellent solubility as well as processability. Interestingly, this membrane became insoluble in any solvent after the thermal treatment [27]. Therefore, this PDMS-graft copolyimide seems to possess an ideal property for membrane material for the use of various applications, such as separation membrane for gases and liquids, because of their excellent processability and durability to several organic solvents.

In this paper, the synthesis of PDMS-graft copolyimides having different PDMS segment length was carried out by the polycondensation of BAPB-PDMS with 6FDA, and the basic characterizations of the copolyimide membranes were investigated. In particular, the influence of the thermal treatment on the membrane characteristics was investigated in detail to clarify the reason why this membrane became insoluble after the thermal treatment, as compared with polyimide derived from 1,3-bis(4-aminophenoxy) benzene and 6FDA. Furthermore, the gas permeability and the pervaporation performance through the obtained PDMS-graft copolyimide membranes were also investigated to reveal the effect of PDMS segment length on the permeability and the selectivity.

2. Experimental

2.1. Materials

3,5-Bis(4-aminophenoxy)benzyloxypropyl-terminated PDMS (BAPB-PDMS) with different PDMS segment length was prepared according to the procedure described in our previous paper [25]. 4,4′-Hexafluoroisopropylidene diphthalic anhydride (6FDA) was purchased from Tokyo Kasei Co., Ltd., and used as received. Anhydrous *N,N*-dimethylacetamide (DMAc) was purchased from Aldrich Co., Ltd. Silicone membrane (thickness: 340 μm) was kindly supplied from Shin-Etsu Chemical Co., Ltd., and used as a reference sample.

2.2. PDMS graft copolyimides (PIS6, PIS11 and PIS19)

The syntheses of PDMS-graft polyimides containing different PDMS segment lengths were performed according to the procedure described in our previous paper [27], as shown in Scheme 1. **PIS6**, **PIS11** and **PIS19** were obtained as a pale brown powder by the reprecipitation of the chloroform solution into excess methanol. ^{1}H NMR and IR spectra of the obtained polymers were added in supporting information as Figs. S1 and S2, respectively. Typical data are shown below.

^{1}H NMR δ ($CDCl_3$, ppm): 0.05 (6(m+1)H, m), 0.53 (4H, m), 0.87 (3H, t, J = 6.63 Hz), 1.30 (4H, m), 1.53 (2H, m), 3.44 (2H, t, J = 6.82 Hz), 4.46 (2H, s), 6.72 (1H, s), 6.86 (2H, s), 7.18 (4H, d, J = 8.73 Hz), 7.38 (4H, d, J = 8.73 Hz), 7.84 (2H, m), 7.96 (2H, s), 8.05 (2H, m).

IR, ν (KBr, cm^{-1}): 2954 (C–H), 1774, 1718 (C=O), 1596, 1583, 1504, 1450, 1371(C–N), 1253 (Si–C), 1213, 1207 1072-1008 (Si–O–Si), 788.

2.3. 1,3-Bis(4-aminophenyloxy)benzene (BAPB)

To a solution of resorcinol (2.50 g, 22.7 mmol), *p*-fluoronitrobenzene (6.72 g, 47.6 mmol) in 50 ml of DMSO and K_2CO_3 (6.57 g, 47.6 mmol) were added. After the mixture was stirred at 140 °C for 15 h, the reaction mixture was poured into excess iced water to precipitate the product. Then, the product was purified by the washing with chloroform to afford 6.81 g of 1,3-bis(4-nitrophenyloxy)benzene as a white powder. Yield: 85.2%.

^{1}H NMR δ ($CDCl_3$, ppm): 6.84 (1H, t, J = 2.43 Hz), 6.79 (2H, d, J = 2.43 Hz), 6.88 (4H, d, J = 8.70 Hz), 7.20 (1H, t, J = 8.29 Hz), 8.17 (4H, d, J = 8.70 Hz).

IR, ν (KBr, cm^{-1}): 3120, 3082, 2935, 2860, 1578, 1506, 1487, 1342 (NO_2), 1223 (C–O–C), 1032, 847.

1,3-bis(4-nitrophenyloxy)benzene (5.0 g, 17.1 mmol) was dissolved in 150 ml of THF/ethanol (1/1 by volume), and Pd/C powder (5%, 0.59 g) was suspended in the solution. Then, the reaction vessel was purged with hydrogen, and the mixture was stirred at room temperature for overnight. After Pd/C powder was filtered off, the product was purified by washing from ethanol for three times to give 4.59 g of 1,3-bis(4-aminophenyloxy)benzene (BAPB) as a white powder. Yield: 92.0%.

^{1}H NMR δ ($CDCl_3$, ppm): 6.35 (3H, m), 6.45 (2H, d, J = 8.29 Hz), 6.58 (4H, d, J = 8.70 Hz), 6.73 (4H, d, J = 8.70 Hz), 7.14 (1H, t, J = 8.29 Hz).

IR, ν (KBr, cm^{-1}): 3403 (NH_2), 2972, 2885, 1570, 1510, 1221 (C–O–C), 1045, 850.

2.4. Polyimide (PI)

Under a nitrogen atmosphere, BAPB (3.30 g, 11.3 mmol) and 6FDA (5.01 g, 11.3 mmol) were dissolved in 47 ml of DMAc. After the solution was stirred for 6 h at room temperature, 4.3 ml of acetic anhydride and 6.3 ml of triethylamine were added, and the mixture was stirred for 10 h at 80 °C. Then, the mixture was poured into excess methanol to precipitate the polymer, and the obtained copolymer powder was filtered and dried. The reprecipitation of the chloroform solution into methanol gave 6.71 g of PI as a white fiber. Yield: 81.3%.

^{1}H NMR δ ($CDCl_3$, ppm): 6.8–6.9 (3H, m), 7.15 (4H, d, J = 8.78 Hz), 7.3–7.4 (1H, m), 7.46 (4H, d, J = 8.78 Hz), 7.88 (2H, s), 7.97 (2H, d, J = 7.80 Hz), 8.07 (2H, d, J = 7.80 Hz).

IR, ν (KBr, cm^{-1}): 2913, 2846 (C–H), 1781, 1720 (C=O), 1587, 1583, 1504, 1371(C–N), 1251, 1205, 1139, 1108, 962, 829, 721.

2.5. Characterizations of polymers

Solution ^{1}H NMR spectroscopy was conducted with a BRUKER AVANCE-500 NMR spectrometer (500 MHz) at room temperature. Infrared (IR) spectra were recorded on a Horiba FT-720 equipped with SensIR technologies DuraSampl*IR* II. Gel permeation

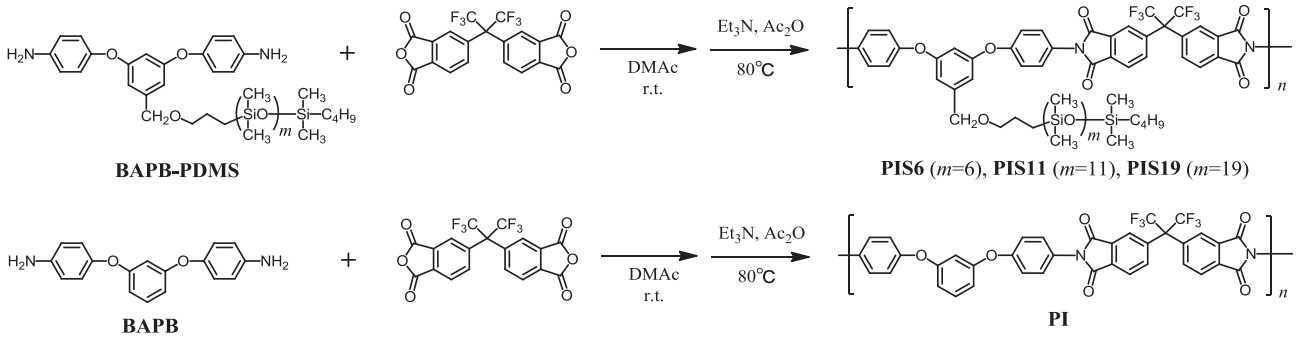

Scheme 1. Syntheses of polyimides.

chromatography (GPC) was carried out to determine the number-average (*M*n) and weight-average (*M*w) molecular weights with a Tosoh HLC-802A instrument by using tetrahydrofuran (THF) as eluent, equipped with four columns of TSK gels $G5000H_6$, $G4000H_6$, $G3000H_6$ and $G2000H_6$. The elution was detected by both of refractive index (RI) and laser light scattering detectors using Tosoh LS-8000 to determine the absolute molecular weight. Standard polystyrenes were used to calibrate the molecular weights. Differential scanning calorimetry (DSC) and thermal gravimetric analysis (TGA) were carried out on Seiko Instruments DSC-6200 and TG/DTA-6200, respectively, at a heating rate of 10 °C min^{-1} under a nitrogen atmosphere.

2.6. Characterizations of polymer membranes

Copolyimide membranes with a thickness of *ca.* 150 μm were prepared by solvent-casting method from the chloroform solutions on the polytetrafluoroethylene sheet and dried at 40 °C for 2 h. To complete the imidization, the thermal treatments of the obtained membranes were carried out at various temperatures, 80 °C, 100 °C, 150 °C, 200 °C and 250 °C, for 24 h. Then, the film samples were cut into rectangular strips with a length of 40 mm and a width of 10 mm. Stress-strain curves of these films were obtained on a JT Torsi LSC-01/30, where the gauge length was 20 mm and the cross-head speed was 6.0 mm min^{-1}.

Sample membranes were cut into circular pieces with a diameter of 14 mm. The density of each membrane was determined by flotation of membrane samples in a density gradient column at 23 °C. Further, the contact angles of ion-exchanged water and ethylene glycol were measured on each membrane surface. The measurements were carried out to use the sessile drop method, and their values were recorded with a Kyowa FACE AUTO DISPENSER AD-31. The reported contact angles are the average value of at least three measurements. According to Owens-Wendt equation [28], the surface free energy was calculated from the values of contact angle of water and ethylene glycol on the membranes.

The membranes were vapor-stained with an aqueous solution of 1 wt% RuO_4 at room temperature for 4 min, and the stained membranes were embedded with epoxy resin at room temperature for 48 h. Thin section of the epoxy-embedded sample was obtained by using an Ultra Microtome (Ultracut UCT: Leica corporation) with a diamond knife. TEM picture was obtained from a Hitachi H7000 operating at 100 kV.

The solid-state ^{13}C- and ^{29}Si CPMAS NMR spectra were measured for thermally treated membranes at 75.5 MHz and 59.6 MHz, respectively, on a BRUKER AVANCE-300 NMR spectrometer (300 MHz for ^{1}H). Samples of ^{13}C and ^{29}Si CPMAS spectra were contained in a cylindrical 2.5 mm and 4 mm zirconia rotor and were spun at 10 kHz and 4 kHz, respectively. ^{13}C and ^{29}Si CPMAS spectra were observed at a contact time of cross polarization of 2 m, a repetition time of 5 s and 10 s, a $\pi/2$ pulse width of 3 μs, and the number of accumulations was 1024. The magic angle was adjusted by using Br signal of KBr, and Hartman-Hahn condition was adjusted by using adamantane and hexamethylcyclotrisiloxane for ^{13}C and ^{29}Si CPMAS spectra, respectively. Up filed peaks of adamantane and hexamethylcyclotrisiloxane were set to be 29.47 ppm and −9.66 ppm from tetramethylsilane, respectively.

2.7. Measurements of gas permeability coefficients

Sample membranes were cut into circular pieces with a diameter of 36 mm. Gas permeability coefficients of the pure gases, *i.e.* hydrogen, oxygen, nitrogen, carbon dioxide and ethane, were measured using the ordinary vacuum method, Tsukuba-Rikaseiki K-315N-01, where the permeation area was 7.07×10^{-4} m^2. The pressures of upstream and downstream sides were about 100 and 0.1 kPa, respectively, and the cell temperature was kept at 30 °C. The gas permeability coefficients (P, m^3 (STP) m m^{-2} s^{-1} Pa^{-1}) were calculated from the slope of the time-pressure curve, dp/dt, in the steady state.

2.8. Pervaporation experiments

Sample membranes were cut into circular pieces with a diameter of 59 mm. Pervaporation of organic liquids/water mixtures through each membrane was carried out using a stainless steel cell, which was dipped in a water bath kept at 50 °C. The pressure of the downstream side was kept at below 0.1 kPa, and the permeation area was 2.0×10^{-3} m^2. The permeated vapor was trapped in a vessel cooled with liquid N_2, and the concentrations of feed and permeate solutions were determined by gas chromatography, using Shimadzu GC-14B and GC-2014 equipped with ZS-72 (3.2 mm × 2.1 m) and G-250 (1.2 mm × 40 m) columns, respectively. The flux (J, kg m^{-2} h^{-1}) was calculated from the weight of permeate (w) in the vessel, the permeation time (t) and the permeation area (A), according to the equations shown below;

$$J = w/At \tag{1}$$

The separation factor, β, was defined as the equation below [29];

$$\beta = (X_{organic}/X_{water})/(Y_{organic}/Y_{water}) \tag{2}$$

where $X_{organic}$ is the mass fraction of organic liquid in permeate, X_{water} is the mass fraction of water in permeate, $Y_{organic}$ is the mass fraction of organic liquid in feed, and Y_{water} is the mass fraction of water in feed.

3. Results and discussion

3.1. Preparations of PDMS-graft copolyimides

Three kinds of PDMS-graft copolyimides (**PIS6**, **PIS11** and **PIS19**) having different PDMS segment length were synthesized by polycondensation of diamino-terminated PDMS macromonomers (BAPB-PDMS) with 6FDA followed by chemical imidization, as shown in Scheme 1. The sample codes of PDMS-graft copolyimides are represented as **PIS*m***, where ***m*** is an average degree of polymerization of PDMS segment in the side chain. Polyimide, **PI**, was prepared by the same procedure from BAPB with 6FDA as a reference sample. PDMS segment length and molecular weights of these polymers are summarized in Table 1. The average degree of polymerization, *m*, of PDMS segment in each graft copolymer was estimated by the ratio of peak intensities of 4.46 ppm (methylene protons in benzyl unit) and 0.05 ppm (methyl protons in PDMS unit) in ^{1}H NMR spectra. As a result, the PDMS segment lengths of these polyimides were in good agreement with those of the starting macromonomers, The obtained copolyimides have the high number-average molecular weights (*M*n) over 2×10^4. Interestingly, the weight-average molecular weights (*M*w) of the graft copolymers determined by GPC were lower than the values of Mw(LS), which were the absolute molecular weight determined by light scattering method. Such branch type polymer usually becomes a compact form in the solution, therefore, the molecular weight determined by GPC mode is known to be smaller than the absolute molecular weight. The obtained PDMS-graft copolyimides were soluble in several organic solvents, such as acetone, chloroform, tetrahydrofuran (THF), toluene and *N*-methylpyrrolidone (NMP), but insoluble in methanol, ethanol and dimethylsulfoxide (DMSO). PI was soluble in chloroform, THF, DMSO and NMP, but insoluble in methanol, ethanol, acetone and toluene.

The thermal properties of these copolymers were evaluated by differential scanning calorimetry (DSC) and thermogravimetric analysis (TGA). It was confirmed from DSC measurements that the thermal transitions of PDMS-graft copolyimides were not observed between −100 °C and 250 °C. The thermal stability of these polymers was evaluated by TGA, as shown in Fig. 1. It was found from TGA curves that the thermal degradation of **PIS6**, **PIS11** and **PIS19** mainly occurred at around 400 °C, whereas that of **PI** occurred over 500 °C. Therefore, it was considered that the weight loss of these copolyimides would be derived from the degradation of the polymer side chain, PDMS segments. Anyway, the heat resistance of these PDMS-graft copolyimides until *ca.* 300 °C seems to be sufficient for the thermal imidization process by heating.

3.2. Characterizations of polymer membranes

The tough self-standing membranes could be prepared by solvent-casting method from the chloroform solutions of PDMS-graft copolyimides, although the low *T*g PDMS chains were included in every repeating units over the content of 50 wt%. In addition, the obtained membranes became insoluble in any solvents by thermal treatment at over 150 °C *in vacuo* for 24 h. The effect of thermal treatment on the membrane properties will be described in the next section.

Table 1
Degree of polymerization of PDMS segment (m) and molecular weights of polyimides.

Code	m^a	$Mn^b \times 10^{-3}$	$Mw^b \times 10^{-3}$	Mw/Mn^b	$Mw(LS)^c \times 10^{-3}$
PIS6	5.7	29.4	94.6	3.22	145
PIS11	11.3	26.0	90.0	3.46	123
PIS19	18.9	27.2	125	4.60	137
PI	–	48.5	112	2.31	125

[a] Average degree of polymerization of PDMS segment (*m*) was calculated by ^{1}H NMR.
[b] Number- and weight-average molecular weights (*M*n and *M*w) were determined by GPC using THF as an eluent.
[c] Mw(LS) was determined by a light scattering detector equipped with GPC.

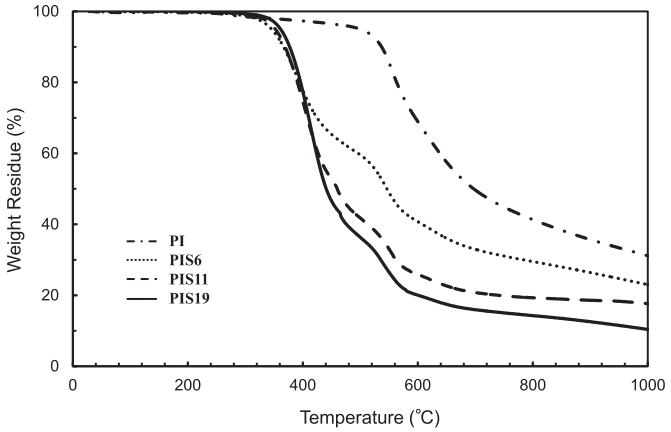

Fig. 1. Thermogravimetric curves of polymer powders.

After thermally treated at 150 °C *in vacuo* for 24 h, the surface property and the density of **PIS6**, **PIS11**, **PIS19** and **PI** membranes were evaluated. The results are listed in Table 2 as compared with silicone membrane. The free surface energy was estimated from the values of contact angle of water and ethylene glycol on the membrane surfaces [28]. The PDMS-graft copolyimide membranes showed the relatively low free surface energy, which would be the evidence that the surface would be effectively covered with PDMS side chain. The free surface energy of silicone membrane was lower than those of copolyimide membranes. Probably, the introduction of polar polyimide backbone made the polymer a little hydrophilic. Hamciuc et al. reported the free surface energy of PDMS/polyimide block copolymers as 51.4 and 61.9 mN m^{-1} estimated by the same method [30], which was higher than those values of PDMS-graft copolyimides. On the other hand, in spite of the rigid backbone, **PIS6**, **PIS11** and **PIS19** membranes showed the lower density than silicone membrane that contained silica filler. These results indicated that the surface property and the density of PDMS-graft copolyimide membranes were affected by the high content of PDMS side chain.

The morphology of **PIS6**, **PIS11** and **PIS19** membrane was investigated by TEM observation. Fig. 2 indicates the TEM images of the cross section of these membranes. In these pictures, the dark region must be PDMS domain stained by RuO_4, because the dark region was increased as the increase of PDMS content. Miyata et al. have studied the morphological effects of microphase separation on the ethanol-permselectivity for the graft copolymer composed of poly(methyl methacrylate) and PDMS [11]. They have described that the PDMS domain was stained by RuO_4, and the permselectivity was strongly governed by the morphology of their microphase separation. Ghosh and Banerjee also reported the micro-phase separation of PDMS/polyimide block copolymer films [31]. As can be seen in Fig. 2, TEM image clearly demonstrated that these membranes consisted of a microphase separation of backbone and side-chain components, and the continuous phase of flexible PDMS domain existed in the membrane, which was surrounded by the hard shell consisted of polyimide backbone. The surface property of the copolyimides would be due to the continuous phase of PDMS domain, and the strength of the membrane would be derived from the polyimide shell.

Table 2
Free surface energy and the density of polymer membranes.

Code	Contact angle (degree)		Free surface energy (mN $m^{-1)}$	Density ($\times 10^{-3}$ kg m^{-3})
	Water	Ethylene glycol		
PIS6	99.2	85.3	14.0	1.189
PIS11	99.2	83.9	14.8	1.153
PIS19	101	82.8	15.8	1.108
PI	92.8	77.0	18.0	–
Silicone[a]	113	106	6.60	1.201

[a] Cross-linked PDMS membrane as a reference sample.

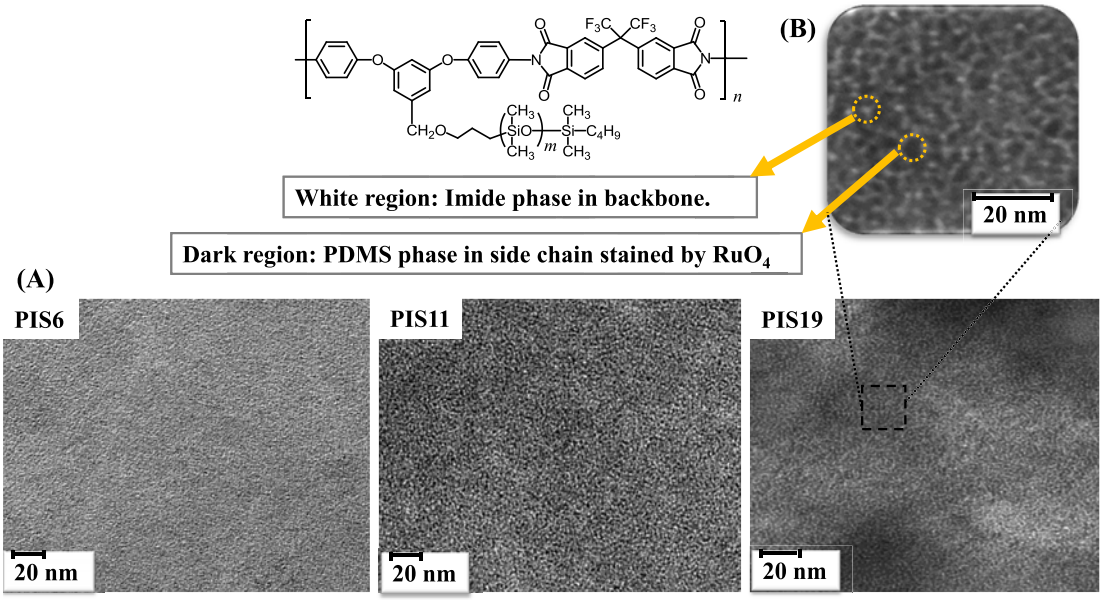

Fig. 2. TEM images of the cross sections of **PIS6**, **PIS11** and **PIS19** membranes stained by RuO_4. (A) Magnification: x 671,000, (B) Magnification: x 1,440,000.

The gas permeabilities of these membranes were investigated to reveal the effect of PDMS segment length on the membrane permeability, which was a basic property for the use of separation membrane. Gas permeability coefficients of N_2, O_2, H_2, CO_2 and C_2H_6 through these membranes were evaluated as shown in Table 3. The gas permeability coefficients of PDMS-graft copolyimide membranes increased as the PDMS segment length became longer (**PIS19** > **PIS11** > **PIS6**), which was in good agreement with the values of density of these membranes listed in Table 2. In addition, CO_2 and C_2H_6 permeability of these membranes were significantly high, although the molecular diameters of these gases were larger than those of the other gases, N_2, O_2 and H_2. The tendency of gas permeability of these copolyimide membranes was similar to that of silicone membrane. Therefore, PDMS-graft copolyimide membranes would possess the highly permeable domains which consisted of PDMS chain with high content.

3.3. Effect of thermal treatment on membrane properties

In general, the thermal imidization process is necessary to complete the conversion of amic acid components to imide bonds even after a chemical imidization in the polymerization, because the small amount of amic acid component is remained in the main chain structure. Actually, the obtained copolyimide films became more substantial after the thermal treatment over 150 °C. However, unexpectedly, it was found that the gas permeability coefficients of

Table 3
Gas permeability coefficients and separation factors of polyimide membranes at 30 °C.

Code	Gas permeability coefficient, *P* (Barrer[a])					Selectivity, P/PN_2			
	N_2	O_2	H_2	CO_2	C_2H_6	O_2/N_2	H_2/N_2	CO_2/N_2	C_2H_6/N_2
PIS6[b]	31.8	80.1	125	469	217	2.52	3.93	14.7	6.82
PIS11[b]	69.7	160	215	900	552	2.30	3.08	12.9	7.92
PIS19[b]	131	292	348	1554	1157	2.23	2.66	11.9	8.83
PI[c]	0.34	1.43	18.4	9.12	$3.1x10^{-3}$	4.21	54.1	26.8	0.01
Silicone[d]	243	509	552	2610	2360	2.09	2.27	10.7	9.71

[a] 1 Barrer = 7.52×10^{-15} m^3 (STP) m m^{-2} sec^{-1} Pa^{-1}.
[b] PIS membranes were heated at 150 °C for 24 h before this measurement.
[c] PI membranes was heated at 250 °C for 24 h before this measurement.
[d] Cross-linked PDMS membrane as a reference sample.

these PDMS-graft copolyimide membranes decreased by the thermal treatment at 200 °C, as shown in Fig. 3. The gas permeability coefficients of nitrogen, oxygen, hydrogen, ethane and carbon dioxide through both of **PIS6** and **PIS11** membranes clearly decreased after the thermal treatments at 200 °C and 250 °C *in vacuo* for 24 h. Therefore, in order to clarify the influence of the thermal treatment on the membrane properties, the changes of mechanical property, IR spectra and CPMAS NMR spectra were investigated for these copolyimide membranes after the thermal treatments at 80 °C - 250 °C.

Fig. 4 shows changes of Young's modulus, the tensile strength and the elongation to break, which are determined by tensile tests of the thermally treated **PI**, **PIS6**, **PIS11 and PIS19** films at each temperature. The stress-strain behaviors of these films are shown in supporting information (Fig. S3 – S6). The values of Young's modulus and tensile strength of **PIS*m*** films slightly increased at 200 °C and 250 °C *in vacuo* for 24 h, where those values of **PI** film similarly increased. On the other hand, the values of elongation to break of **PIS*m*** films decreased at 200 °C treatment *in vacuo* for 24 h, whereas the elongation of **PI** film slightly increased. It was considered that the imidization of the small amount of amic acid component proceeded in every films at over 150 °C *in vacuo* for 24 h, which resulted in the increase of Young's modulus and tensile strength. Anyhow, the great decrease of elongation values of **PIS*m*** films, as shown in Fig. 4 (C), would be caused by the other factors, for example, the change of soft segment, *i.e.* PDMS segment in the side chain.

Accordingly, FT-IR spectra and ^{13}C and ^{29}Si CPMAS spectra were measured for thermally treated films to reveal the change in chemical structure of **PIS6** film, which exhibited the greatest change in the gas permeability and the elongation to break. Fig. 5 (A) shows the difference of FT-IR spectra of **PIS6** films after treated at 100 °C and 250 °C *in vacuo* for 24 h. Then, the ratios of peak intensities of PDMS segment (Si–C and Si–O–Si) and the carbonyl group in the backbone component (C=O) of **PIS6** were calculated from the FT-IR spectra. Fig. 5 (B) shows the relationship between the temperature of thermal treatment and the ratios of peak intensities in FT-IR spectra of **PIS6** film. The intensity ratio of Si–C and Si–O–Si/C=O were estimated from the absorption peak intensities at 1253 cm^{-1} (Si–CH_3 δ), 1012 cm^{-1} (Si–O–Si st) and 1722 cm^{-1} (C=O st). As a standard value, the intensity ratio of Ar/C=O was also calculated from the absorption peak intensities at 1504 cm^{-1} (C=C st in aromatic ring) and 1722 cm^{-1}. As seen in Fig. 5 (B), according to the thermal treatment at 200 °C and 250 °C *in vacuo* for 24 h, the intensity ratios of Si–C/C=O and Si–O–Si/C=O were definitely decreased, although the ratio of Ar/C=O was not changed. Hence, it is speculated that PDMS segment was reduced by the thermal treatment at 200 °C.

^{13}C and ^{29}Si CPMAS NMR spectra were conducted for the thermally treated **PIS6** films at various temperatures, as shown in Fig. 6. In Fig. 6 (A), the peaks between 100 ppm and 170 ppm were assigned to aromatic carbons in the backbone component of **PIS6**, and the peaks at 20–30 ppm were assigned to the terminal $-C_4H_9$ groups in PDMS segments. A peak at 0 ppm is assigned to the $-CH_3$ groups of PDMS components. It was observed in Fig. 6 (A) that the peak intensities at 20–30 ppm and 0 ppm decreased as the temperature increased from 150 °C to 250 °C, when those were compared to the peak intensities at 100–170 ppm. This result suggested that the backbone structure was not affected by the thermal treatment, but the thermal elimination of the $-C_4H_9$ end group in PDMS segment occurred and the reduction of PDMS segments proceeded especially at 250 °C. In addition, as shown in Fig. 6 (B), the peak intensity at 9 ppm was significantly affected by thermal treatment, where the peaks at 9 ppm and −24 ppm were assigned to -$Si(CH_3)_2$–C_4H_9 and -$Si(CH_3)_2$O-, respectively. The peak intensity of the terminal silyl group (9 ppm) of PIS6 film treated at 200 °C or 250 °C was obviously lower than that treated at 80 °C or 150 °C, while the peak intensities of the siloxane unit (−24 ppm) were observed without change. This NMR results indicated that the component of terminal butyldimethylsilyl group in PDMS segment was decreased by the thermal treatment at 200 °C and 250 °C *in vacuo* for 24 h.

From these results, it would be demonstrated that a cross-linked reaction occurred between the PDMS segments in the side chain during the thermal treatment at nearly 200 °C *in vacuo* for 24 h, where the elimination of terminal group of PDMS segment occurred as an initiation reaction. The speculated reaction mechanism is shown in Fig. 7. The rearrangement of PDMS chain would occur by acidic atmosphere in the presence of the very small amount of unreacted amic acid unit during the chemical imidization, even though it was not observed in ^1H NMR and FT-IR spectra. Unfortunately, this phenomenon was not confirmed as a weight

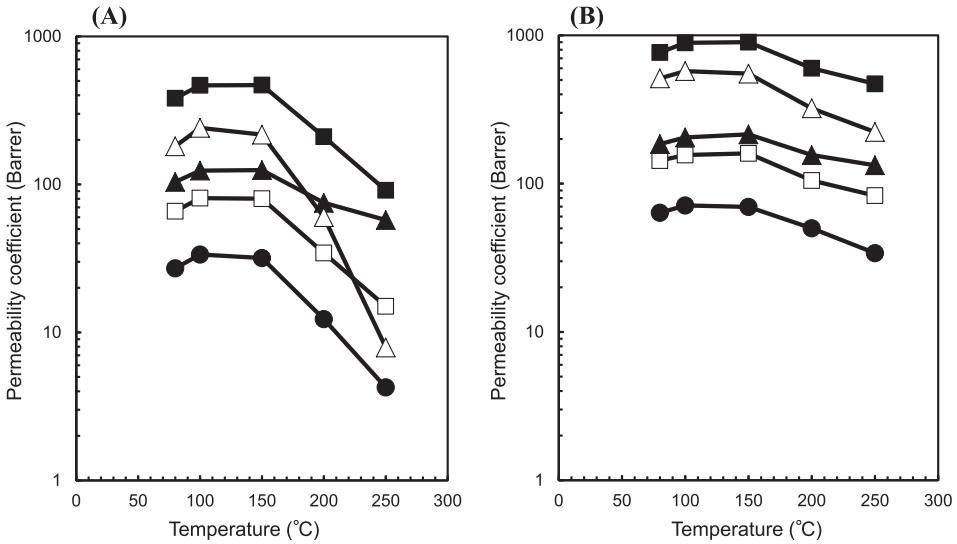

Fig. 3. The effect of temperature of the thermal treatment on the gas permeability coefficients of nitrogen (●), oxygen (□), hydrogen (▲), ethane (△) and carbon dioxide (■) through (A) **PIS6** and (B) **PIS11** membranes.

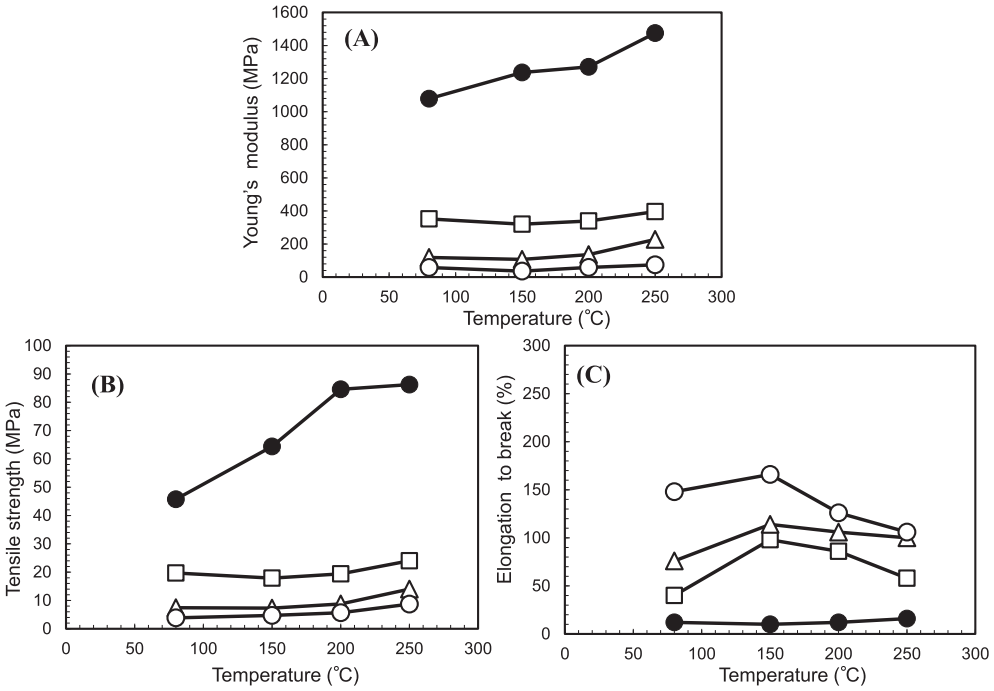

Fig. 4. The effect of temperature of the thermal treatment on (A) Young's modulus, (B) tensile strength and (C) elongation to break of **PI** (●), **PIS6** (□) and **PIS11** (△) films.

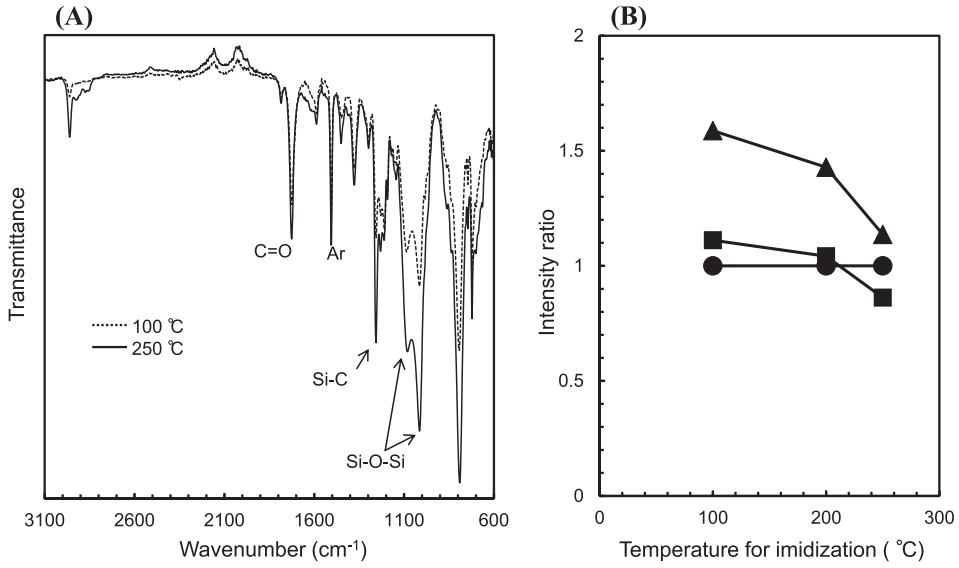

Fig. 5. (A) FT-IR spectra of **PIS6** film after thermally treated at 100 °C and 250 °C *in vacuo* for 24 h. (B) Relationship between the temperature of thermal treatment and the intensity ratios of peak intensities in FT-IR spectra of **PIS6** film. ▲: Si–C/C=O, ■: Si–O–Si/C=O, ●: Ar/C=O.

loss in TGA measurement from 200 °C to 250 °C (Fig. 1), which would be due to the difference of heating condition. Then, the cross-linking of the side chain proceeded in the thermal treatment to make the membrane insoluble. Therefore, it was considered that the PDMS-graft polyimide membrane was expected to be an ideal material for pervaporation membrane, because of its good processability and the durability to several organic liquids.

3.4. Pervaporation performance

The effect of PDMS segment length on the pervaporation performance of PDMS-graft copolyimide membranes, which were thermally treated at 200 °C *in vacuo* for 24 h, was investigated as compared with silicone membrane. The dilute aqueous solutions of organic liquids, such as ethanol, acetone, benzene, chloroform and dichloromethane, were used as feed solutions in the pervaporation experiments. The saturated organic solutions in water were prepared for benzene, chloroform and dichloromethane. The pervaporation results of each membrane are summarized in Table 4.

As a result, the preferential permeation of organic liquids was observed for all the membranes, and the separation factor and the flux increased as the increase of PDMS segment length. Such an organic-permselectivity would be due to the high solubility of the organic solvents on the membrane surface and the high diffusivity

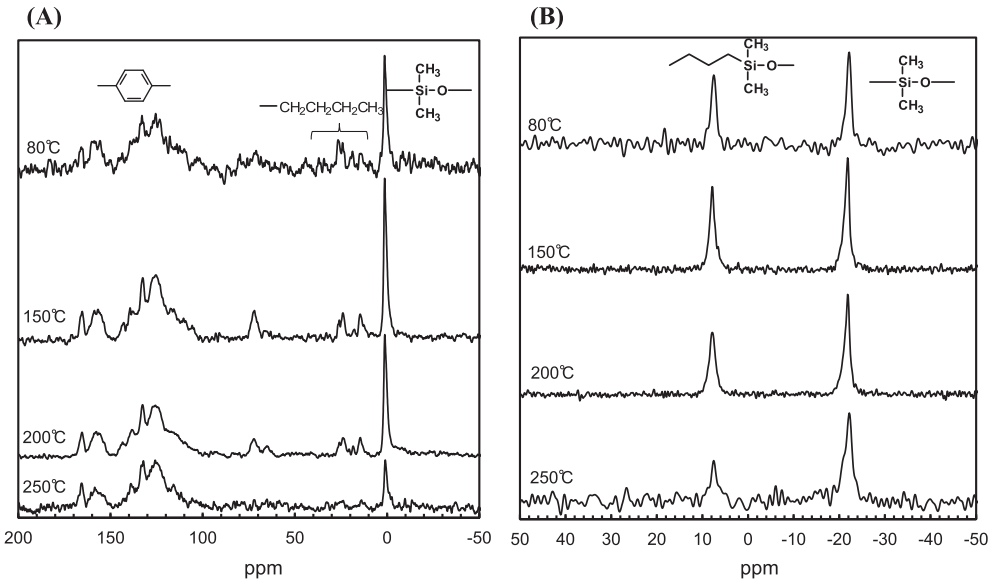

Fig. 6. (A) ^{13}C and (B) ^{29}Si CPMAS NMR spectra of **PIS6** film after thermally treated at various temperatures, 80 °C, 150 °C, 200 °C and 250 °C, *in vacuo* for 24 h.

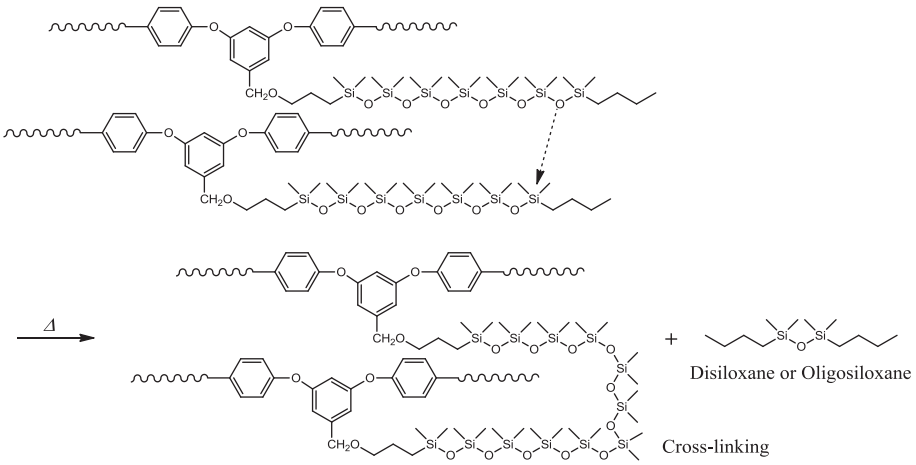

Fig. 7. Speculated cross-kinking reaction mechanism by thermal treatment.

through the membrane. The high diffusivity of the membrane would be an important factor to achieve the organic-selectivity in pervaporation, because the difference between the diffusivities of the relatively large organic molecules and the small water molecule should be minimized throughout the membrane. On the other hand, it was reported that the difference of selectivity for each organic liquid through such organic-permselective membrane was strongly depended on the solubility parameters of organic liquids [25]. For example, *ca.* 9.5 wt% aqueous solutions of ethanol and acetone were concentrated to 50 wt% and 81 wt%, respectively, through **PIS19** membrane. On the contrary, in the pervaporation of benzene, chloroform and dichloromethane solutions, **PIS11** and **PIS19** membranes exhibited very high separation factors, which were higher than that of silicone membrane. Especially, the saturated solution of dichloromethane in water (2.0 wt%) was concentrated to nearly 90 wt% through **PIS11** and **PIS19** membranes. It would be due to the high solubility of the dichloromethane on the membrane surface, the solubility parameter of which should be almost same as that of dichloromethane. Therefore, it is expected that these membranes have a great advantage for the removal of VOCs such as dichloromethane, chloroform and benzene, whose environmental standards are very strict for waste fluid or industrial drainage.

Concerning the application to a removal of VOCs from their dilute aqueous solutions, the removal efficiency of dichloromethane from its dilute aqueous solution was investigated by the similar pervaporation experiment using **PIS6**, **PIS11**, **PIS19** and silicone membranes. For this purpose, the feed concentrations were determined by gas chromatography in 5 h intervals during the pervaporation of 400 g of the saturated dichloromethane solutions in water. The changes in the feed concentrations are shown in Fig. 8. These **PIS*m*** membranes exhibited the better efficiency than silicone membrane, which would be due to the difference of membrane thickness as listed in Table 4. It was found that the concentration of dichloromethane was efficiently reduced by the pervaporation through these membranes with a stable permeation during 10 h, where 1.8 wt% of dichloromethane was reduced to 0.08 wt% in the case of **PIS11** membrane. Kujawski et al. have also reported the detailed experiments for the effective removal of acetone, butanol and ethanol from the dilute aqueous solutions by pervaporation through PDMS membrane [3]. Thus, if the ultrathin membrane can be produced on a porous support membrane, it is

Table 4
Pervaporation of dilute aqueous organic liquids through PIS9, PIS11, PIS19 and silicone membranes at 50 °C. (Thickness: PIS6, PIS11, PIS19 = 150 mm, Silicone = 340 mm).

Code	Organic liquid	Composition[a](wt%)		β^b	$J^b \times 10^2$ (kg m^{-2} h^{-1})
		In feed	In permeate		
PIS6	Ethanol	9.24	25.2	3.30	1.63
PIS11		9.26	40.5	6.66	3.00
PIS19		9.53	50.0	9.49	5.72
Silicone[c]		9.60	51.1	9.80	2.69
PIS6	Acetone	9.73	60.5	13.0	3.98
PIS11		9.73	74.5	25.0	10.8
PIS19		9.75	80.7	38.7	15.2
Silicone[c]		9.86	81.5	40.3	8.36
PIS6	Benzene	0.20	34.0	258	2.21
PIS11		0.20	39.5	325	4.30
PIS19		0.20	45.2	412	4.84
Silicone[c]		0.20	39.8	330	2.97
PIS6	Chloroform	0.80	62.3	205	4.31
PIS11		0.80	70.1	291	8.49
PIS19		0.80	67.2	254	9.04
Silicone[c]		0.80	66.9	250	5.52
PIS6	Dichloromethane	2.00	86.5	315	9.38
PIS11		2.00	89.6	420	28.2
PIS19		2.00	89.4	413	29.4
Silicone[c]		2.00	87.7	349	17.1

[a] Composition of organic liquid in feed and permeate.
[b] β: Separation factor (organic liquid/water), J: Flux.
[c] Cross-linked PDMS membrane as a reference sample.

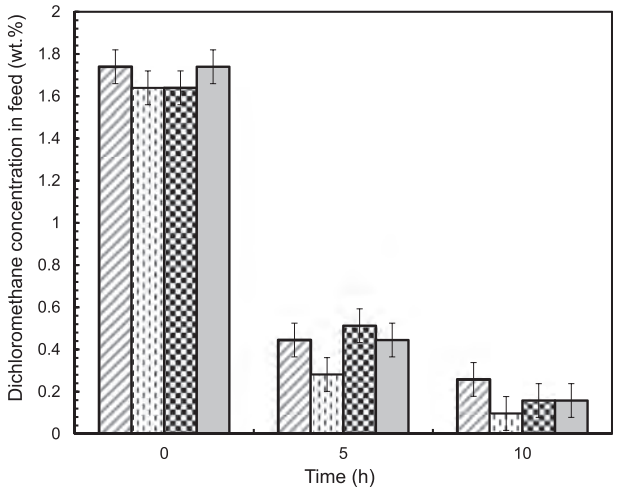

Fig. 8. Changes in the feed concentrations in the pervaporation of saturated dichloromethane solution in water through **PIS6** (diagonal line), **PIS11** (dotted line), **PIS19** (checkerboard) and silicone (dark gray) membranes. Amount of feed solution: 400 g, Permeation area: 2.0×10^{-3} m^2.

expected that a removal of organic components from waste fluid or fermentation broth would be efficiently achieved.

When these membranes were swollen with feed solutions in pervaporation, it was wondering that the microphase separation as shown in Fig. 2 might be changed to reduce the separation performance. However, the hard shell consisted of polyimide backbone would work as the linkage of PDMS domain to maintain the stable permeation during pervaporation. Actually, it was demonstrated that the gas permeability of dried **PIS11** membrane, which was once used in pervaporation experiment, was not different from that of virgin membrane and the reproducibility of pervaporation results was also observed. Therefore, such a microphase separation of PDMS and polyimide phases would be stable enough for the membrane to achieve the stable permeations of gases and liquids.

4. Conclusion

Three kinds of PDMS-graft copolyimides having different PDMS segment lengths were successfully synthesized, and the tough self-standing membranes were prepared by solvent casting method, which became insoluble in any solvent by thermal treatment at over 150 °C. From the detailed characterizations of the thermally treated membranes, it was speculated that the rearrangement of PDMS segments occurred according to the elimination of the terminal silyl group, which resulted in the cross-linked structure between the PDMS segments to make the membrane insoluble. It was also found from TEM observations that these membranes consisted of a microphase separation of backbone and side-chain components to produce a honeycomb-like structure, where the flexible PDMS domain was surrounded by the hard shell consisted of polyimide backbone. The high gas permeability of the membrane would be caused by the continuous phase of flexible PDMS domain, and the mechanical strength would be derived from the hard shell. Furthermore, the pervaporation performance of these membranes induced the efficient removal of VOCs from the aqueous mixtures. Consequently, it is expected that PDMS-graft copolyimide membrane can be used for the removal of toxic organic components from the waste-water by pervaporation technique, due to their enough permselectivity, processability for the production of thin membrane and durability to organic liquids.

Acknowledgment

The authors would like to thank Dr. Takamasa Fuchikami and Dr. Takamasa Yoshida, who belong to Chemicrea Co., Ltd., for their help of the determination of the dilute concentrations of dichloromethane by gas chromatography. We also express our gratitude to Professor Tomokazu Iyoda and Assistant Professor Kaori Kamata, who belong to Chemical Resources Laboratory, Tokyo Institute of Technology, for their help in TEM observations. Then, we sincerely thank Professor Takashi Asaka, who belongs to Department of Applied Chemistry, Tokai University, for his help in the measurements of stress-strain behaviors of polymer films. This work was supported by a Grant-in-Aid for Research from the Tokai University

Support Association Union.

Appendix A. Supplementary data

Supplementary data related to this article can be found at http://dx.doi.org/10.1016/j.polymer.2016.09.044.

References

[1] I. Blume, J.G. Wijmans, R.W. Baker, J. Membr. Sci. 49 (1990) 253–286.
[2] S. Claes, P. Vanderzande, S. Mullens, K.D. Sitter, R. Peeters, M.K. Van Bael, J. Membr. Sci. 389 (2012) 265–271.
[3] J. Kujawski, A. Rozicka, M. Bryjak, W. Kujawski, Sep. Purif. Technol. 132 (2014) 422–429.
[4] M. Karaszova, M. Kacirkova, K. Friess, P. Izak, Sep. Purif. Technol. 132 (2014) 93–101.
[5] A. Kujawska, J. Kujawski, M. Bryjak, W. Kujawski, Renew. Sustain. Energy Rev. 48 (2015) 648–661.
[6] S. Kimura, T. Nomura, Membrane 8 (1983) 177–183.
[7] T. Ohshima, T. Miyata, T. Uragami, H. Berghmens, J. Mol. Str. 739 (2005) 47–55.
[8] X. Han, L. Wang, J. Li, X. Zhan, J. Chen, J. Yang, J. Appl. Polym. Sci. 119 (2011) 3413–3421.
[9] A. Rozicka, J. Niemisto, R.L. Keiski, W. Kujawski, J. Memb. Sci. 453 (2014) 108–118.
[10] K. Okamoto, A. Butsuen, S. Tsuru, K. Tanaka, H. Kita, S. Asakawa, Polym. J. 19 (1987) 747–756.
[11] T. Miyata, H. Yamada, T. Uragami, Macromolecules 34 (2001) 8026–8033.
[12] S. Chovau, A. Dobrak, A. Figoli, F. Galiano, S. Simone, E. Drioli, S.K. Sikdar, B.V. Bruggen, Chem. Eng. J. 159 (2010) 37–46.
[13] P.A. Gurr, J.M. Scofield, J. Kim, Q. Fu, Kentish, G.G. Qiao, J. Polym. Sci. Polym. Chem. Ed. 52 (2014) 3372–3382.
[14] T. Uragami, Y. Matsuoka, T. Miyata, J. Memb. Sci. 506 (2016) 109–118.
[15] J.M.P. Scofield, P.A. Gurr, J. Kim, Q. Fu, S.E. Kentish, G.G. Qiao, J. Memb. Sci. 499 (2016) 191–200.
[16] S.V. Kumar, C. Arnal-Herault, M. Wang, J. Babin, A. Jonquieres, ACS Appl. Mater. Interfaces 8 (2016) 16262–16272.
[17] T.L. St. Clair, in: D. Wilson, H.D. Stenzenberger, P.M. Hergenrother (Eds.), Polyimide, Springer, New York, 1990, pp. 58–78. Chapter 3.
[18] T. Taikoshi, in: M.K. Ghosh, K.L. Mittal (Eds.), Polyimides: Fundamentals and Applications, Marcel Dekker, New York, 1996, pp. 7–48. Chapter 2.
[19] S.A. Stern, J. Membr. Sci. 94 (1994) 1–65.
[20] N. Schmeling, R. Konietzny, D. Sieffert, P. Rolling, Beilstein J. Org. Chem. 6 (2010) 789–800.
[21] S. Xu, Y. Wang, J. Membr. Sci. 496 (2015) 142–155.
[22] Y. Nagase, S. Mori, M. Egawa, K. Matsui, Makromol. Chem. 191 (1990) 2413–2421.
[23] E. Akiyama, Y. Takamura, Y. Nagase, Makromol. Chem. 193 (1992) 1509–1519.
[24] E. Akiyama, Y. Takamura, Y. Nagase, Makromol. Chem. 193 (1992) 2037–2047.
[25] Y. Nagase, T. Ando, C.M. Yun, React. Func. Polym. 67 (2007) 1252–1263.
[26] C.M. Yun, Y. Saito, Y. Nagase, Trans. Mater. Res. Soc. Jp. 33 (2008) 1265–1268.
[27] C.M. Yun, A. Abeta, S. Wirittichai, K. Yamamoto, H. Ishikura, Y. Nagase, Trans. Mater. Res. Soc. Jp. 35 (2010) 237–240.
[28] D.K. Owens, R.C. Wendt, J. Appl. Polym. Sci. 13 (1969) 1741–1747.
[29] R.W. Baker, J.G. Wijmans, Y. Huang, J. Memb. Sci. 348 (2010) 346–352.
[30] E. Hamciuc, C. Hamciuc, M. Cazacu, M. Ignat, G. Zarnescu, Eur. Polym. J. 45 (2009) 182–190.
[31] A. Ghosh, S. Banerjee, J. Appl. Polym. Sci. 107 (2008) 1831–1841.